



Published in final edited form as:

J Urol. 2017 October ; 198(4): 780–786. doi:10.1016/j.juro.2017.04.089.

Diagnostic Accuracy of Multiparametric Magnetic Resonance Imaging to Identify Clear Cell Renal Cell Carcinoma in cT1a Renal Masses

Noah E. Canvasser¹, Fernando U. Kay², Yin Xi², Daniella F. Pinho², Daniel Costa², Alberto Diaz de Leon², Gaurav Khatri², John R. Leyendecker², Takeshi Yokoo², Aaron Lay¹, Nicholas Kavoussi¹, Ersin Koseoglu¹, Jeffrey A. Cadeddu^{1,2}, and Ivan Pedrosa^{2,3}

¹Department of Urology, University of Texas Southwestern, Dallas, TX

²Department of Radiology, University of Texas Southwestern, Dallas, TX

³Advanced Imaging Research Center, University of Texas Southwestern, Dallas, TX

Abstract

Purpose—Detection of small renal masses is increasing with the use of cross-sectional imaging, although many incidental lesions have negligible metastatic potential. Among malignant masses, clear cell renal cell carcinoma is the most prevalent and aggressive subtype, and a method to identify such histology would aid in risk stratification. Our goal was to evaluate a likelihood scale for multiparametric magnetic resonance imaging in the diagnosis of clear cell histology.

Methods—Patients with cT1a masses who underwent MRI and partial or radical nephrectomy from December 2011 to July 2015 were retrospectively reviewed. Seven radiologists with different levels of experience and blinded to final pathology independently reviewed studies based on a predefined algorithm, and applied a clear cell likelihood score: 1) definitely not, 2) probably not, 3) equivocal, 4) probably, and 5) definitely. Binary classification determined the accuracy of clear cell versus ‘all other’ histologies, and inter-observer agreement was calculated with a weighted κ statistic.

Results—In total, 110 patients with 121 masses were identified. Mean tumor size was 2.4 cm and 50% were clear cell. Defining clear cell as scores ≥ 4 demonstrated sensitivity and specificity of 78% and 80%, respectively, while scores ≥ 3 were 95% and 58%, respectively. Inter-observer agreement was moderate to good, with a mean κ of 0.53.

Conclusions—A clear cell likelihood score with MRI can reasonably identify clear cell histology in small renal masses, and may reduce the number of diagnostic renal mass biopsies. Standardization of imaging protocols and reporting criteria are needed to improve inter-observer reliability.

*Correspondence: Jeffrey A. Cadeddu, MD, Department of Urology, University of Texas Southwestern Medical Center, 5323 Harry Hines Blvd, Dallas, TX 75390-9110, 214-648-2888, FAX: 214-648-8786, jeffrey.cadeddu@utsouthwestern.edu.

Institutional Review Board approval: Yes

Keywords

kidney neoplasms; carcinoma; renal cell; MRI

Introduction

Approximately one quarter of small renal masses (SRM) less than 4 cm are histologically benign.¹ However, the role of percutaneous biopsy in the management of SRM remains controversial.² Recent evidence indicates that while renal mass biopsy (RMB) is highly accurate in renal cell carcinoma (RCC) diagnosis,³ multiple studies demonstrate underutilization.^{4,5} Potential explanations include that RMB is an invasive procedure with a 1.4%–4.7% complication rate,³ fails to provide diagnostic information for malignancy in 14% of cases,⁶ and is unreliable in tumor grade determination.³

Based on excellent soft-tissue contrast and a combination of qualitative, semi-quantitative, and quantitative characteristics, multiparametric magnetic resonance imaging (mpMRI) can histologically subtype renal cell carcinoma (RCC).^{7–10} As an alternative to computed tomography, mpMRI could potentially provide both histologic and anatomic information prior to therapeutic intervention, obviating the need for biopsy or additional imaging. However, literature pertaining to the clinical applicability of mpMRI to define higher-risk RCC in SRM is sparse.^{7,11–13} Furthermore, to our knowledge, the inter-observer reproducibility between more than three reviewers in mpMRI evaluation of RCC has not been reported.^{12–14}

Clear cell RCC (ccRCC) is the most common RCC variant and notably potentially aggressive.¹⁵ On MRI it is characterized by heterogeneous high signal intensity on T2-weighted imaging,¹⁰ presence of microscopic fat,^{16–19} and avid enhancement equal to or greater than renal cortex.¹¹ Given that the probability of ccRCC diagnosis is proportional to the added effect of individual parameters, a likelihood score based on those MRI parameters might provide a useful tool for patient management, as has been done with prostate cancer.^{20,21}

Our goal was to evaluate the diagnostic accuracy of a subjective likelihood scale for mpMRI in the diagnosis of ccRCC in cT1a lesions and to assess the inter-reader reproducibility of such scale.

Materials and Methods

Patients

This retrospective series was performed under Institutional Review Board approval. Patients with cT1a renal masses who underwent either partial or radical nephrectomy and pre-surgical mpMRI between December 2011 and July 2015 were identified. Patients with poor quality or limited MRI examinations (n=3) (i.e. not including the sequences described below) were excluded from analysis. Patient demographics and clinical findings including age, sex, tumor size, and final pathology were extracted from chart review. Histologic

analysis was performed by genitourinary pathologists according to the World Health Organization classification of renal neoplasms.²²

Image Acquisition

mpMRI studies were performed on 1.5T and 3.0T scanners from multiple institutions with diverse parameters, as many patients underwent mpMRI elsewhere and were referred to the authors' institution for treatment. In total, 54 patients (49%) had imaging at our institution, while 56 patients (51%) had imaging obtained elsewhere. An MRI fellowship-trained radiologist (blinded), who was not involved in imaging interpretation, reviewed all mpMRI exams of patients in this study to ensure they were of sufficient image quality and basic sequences were included. At the authors' institution mpMRI includes the following sequences: T2-weighted images in coronal and axial (with fat-suppression) planes (4–8mm slice thickness, 256×154 to 348×280 matrix, 70–120ms echo time (TE), and 964–4820ms repetition time (TR)), axial chemical shift T1-weighted images (5–8mm thickness, 193×168 to 500×286 matrix, 2.38/4.87ms (1.5T) or 1.1/2.3ms (3.0T) TE, and 100–216ms TR), and fat-suppressed dynamic contrast-enhanced (DCE) T1-weighted imaging, including corticomedullary and late nephrographic and/or excretory phases in either axial or coronal planes (3–6mm slice thickness, 176×149 to 320×259 matrix size, 1.6–2.4ms TE, and 3.4–5.4ms TR). Diffusion weighted images (DWI) were routinely acquired at the authors' institution but inconsistently present in mpMRI studies performed elsewhere so these were not evaluated. Furthermore, given the controversial role of DWI in characterizing renal masses and the importance of acquisition protocol standardization,²³ these images were not included in the analysis.

Image Analysis

Seven radiologists with fellowship training in body MRI from a single institution with a busy MRI service (approximately 7,000 abdominopelvic MRIs/year), varying levels of experience (IP and JRL 15 years, DC 12 years, TY 10 years, GK 7 years, DC 5 years, ADL 1 year), and blinded to final pathology, independently reviewed each study on a PACS workstation (iSite, Philips Healthcare, Best, Netherlands). A Likert scale was used to convey the subjective radiologic impression of the likelihood of encountering ccRCC at surgery. The clear cell likelihood score (ccLS) was defined as: 1) definitely not ccRCC, 2) probably not ccRCC, 3) equivocal for ccRCC, 4) probably ccRCC, and 5) definitely ccRCC. "Cannot be assessed" was also allowed if perceived inadequacy of the MRI protocol. Prior to image analysis, all radiologists received a refresher training session with a slide presentation including examples of the main imaging features associated with ccRCC histology and other common histologic diagnoses in renal masses. A detailed review of such features is published elsewhere (figure 1).²⁴ Each reader was allowed to measure signal intensity using region of interest (ROI) analysis, and quantify the corticomedullary enhancement¹¹ and arterial-delayed enhancement ratio per individual judgment.²⁵ For statistical purposes, a composite ccLS was calculated as a mean of the seven readers when appropriate.

Statistical Analysis

Scoring each renal mass for ccRCC diagnosis was compared to the reference standard, which was determined by histology (ccRCC vs. 'all other' histologies). Receiver operating

characteristic (ROC) analysis was performed to calculate the area under the curve (AUC) and corresponding 95% confidence interval for each reader. Tumors that could not be assessed were excluded from ROC analysis. Multiple comparisons in mean AUCs among readers were performed with a Bonferroni correction. Pairwise inter-observer agreement was assessed by weighted κ statistics. A p-value of 0.05 or less was considered statistically significant. All statistical analysis was performed with SAS version 9.4 (SAS Institute Inc., Cary, NC, USA).

Results

In total, 110 patients with 121 cT1a renal masses were identified. Patient demographics and final pathologic findings are shown in table 1. Mean tumor size was 2.4 cm (range 0.5–4.0 cm), and histology was ccRCC in 50% (n=61), non-clear cell RCC in 33% (n=40), and benign lesions in 17% (n=20).

Histologic distribution of the entire cohort by ccRCC versus ‘all other’ histologies and assigned ccLS is shown in figure 2, while overall comparison of ccLS score to final histology is shown in table 2. Overall, a mean of 2.8 tumors (2.3%) could not be assessed by reviewers. Tumors with ccLS 4–5 were categorized as mpMRI-identified ccRCC (MR-ccRCC). Combining all seven readers gave a mean accuracy of 79%, sensitivity of 78%, specificity of 80%, positive predictive value (PPV) of 80%, and negative predictive value (NPV) of 80% (figure 3). Augmenting the MR-ccRCC definition to include ccLS 3 tumors changed the mean accuracy to 77%, sensitivity to 95%, specificity to 58%, PPV to 70%, and NPV to 93%, which inversely gave ccLS 1–2 a specificity of 95% and PPV of 93% for ‘all other’ histologies.

Among all readers, a mean of 12.2 tumors (10.1%) were false positive ccLS 4–5 lesions. The most common false positive histology was oncocytoma (mean 2.7 tumors, 22.1%) followed by papillary RCC (mean 1.3 tumors, 10.7%), chromophobe RCC (mean 1 tumor, 8.2%) and lipid-poor angiomyolipoma (AML) (mean 0.9 tumors, 7.4%). A mean of 2.7 tumors (2.2%) per reader were false negative ccRCC tumors graded as ccLS 1–2; 50% without high signal intensity on T2-weighted imaging, 79% without high contrast avidity, 100% without intravoxel fat, and 84.2% without central scar, which suggested against higher scoring.

ROC curves for the seven readers are shown in figure 4, with AUC ranging from 0.82–0.92. Comparisons of the highest rated reader (Reader 7, AUC 0.92) compared to all other readers showed a statistically significant difference between all readers except reader #4, and years of experience did not correlate with improved diagnostic accuracy (p=0.31). Inter-reader variability was moderate to good, with a mean weighted κ of 0.53 (range 0.38–0.64).

Discussion

Multiparametric MRI is an appealing alternative to RMB, in that it can provide both pathologic information to direct management and anatomic information required for surgical planning. To our knowledge, our series is the first to specifically evaluate the diagnostic accuracy of mpMRI for ccRCC in cT1a lesions. The proposed ccRCC likelihood scoring system demonstrated a high specificity and PPV for ccRCC in ccLS 4–5 lesions, and a high

specificity (95%) and PPV (93%) for non-ccRCC in ccLS 1–2 lesions, in addition to moderate inter-observer reliability. Therefore, ccLS could support an algorithm where all ccLS 4–5 are encouraged to undergo curative interventions, all ccLS 1–2 are placed on active surveillance (especially if they are less than 3 cm), and only ccLS 3 undergo RMB. This proposal would result in a biopsy rate in this series of only 20%, unnecessary treatment of oncocytoma and lipid-poor AML in 4.5% and 1.7% of the surgical cohort, respectively, and 4.4% of ccRCC placed on active surveillance. It should be noted that ccLS was not a good predictor of overall malignancy. This is expected since it was developed for ccRCC diagnosis. Accordingly, while most ccRCCs received a high score, most non-clear cell RCCs were assigned a low score.

In one of the first studies to evaluate a comprehensive classification of renal masses with mpMRI, Pedrosa et al. defined eight distinct qualitative mpMRI patterns of malignant lesions among T2-, chemical shift T1-, and contrast enhanced T1-weighted sequences.⁷ They reported that two radiologists demonstrated a slightly higher sensitivity and specificity of 92% and 83%, respectively, compared to our series for diagnosing ccRCC. Of these 48 ccRCC tumors mean tumor size was much larger than the present series (6.0 cm), and they excluded benign lesions, which may explain the slightly higher accuracy. Cornelis and colleagues compared mpMRI of 100 renal masses to pathologic findings, and noted high specificity for diagnosing papillary RCC and oncocytomas.¹² Differing from our study, they included significant parameters quantified by two radiologists, and all RCC subtypes were mean >4.0 cm. Recently, Hötter and colleagues published their evaluation of 124 renal masses by MRI compared to pathologic findings.¹³ Although the median tumor size of their ccRCC cohort (n=81) was 8.0 cm, they noted that the apparent diffusion coefficient, peak enhancement, and downslope of DCE sequence significantly correlated with ccRCC histology. In addition, after two independent radiologist's review they noted significant interreader agreement (r= 0.82–0.99).

Despite other investigators use of mpMRI in large (>4.0 cm) renal tumors, in the context of clinical practice we feel the most relevant use of mpMRI is in classification of SRM (<4.0 cm). In a database of over 2700 patients, Frank and colleagues noted that 23% of tumors <4.0 cm were pathologically benign, compared to only 8% of tumors ≥ 4.0 cm.²⁶ Therefore, the current role of RMB is in identifying SRM histology to plan surgical intervention or active surveillance.²⁷ Recent meta-analysis of RMB have demonstrated low false positive and false negative rates of 4.0% and 3.1%, respectively, in addition to low complication rates (4.9% hematoma and 1.2% pain).⁶ However, as previously mentioned, this is in the context of a 14% non-diagnostic rate. In addition, histologic grade concordance between biopsy and final pathology was 52–76%. In comparison, our mpMRI results demonstrated false-positive and false negative rates of 6.2% and 4.4%, respectively, no complications, and a 2.3% non-diagnostic rate. As for tumor grade, we did not analyze grade concordance in this initial series. Prior work has looked at differentiating high grade and low grade ccRCC in large tumors with good success.⁷ The ability to do so in smaller tumors is unknown, but likely more difficult.

Additionally, many RMB studies carried selection bias as percutaneous biopsy may not be easily performed and/or may carry worse outcomes (e.g. lower diagnostic yield, increased

complications) in those patients with SRMs in difficult anatomic locations (e.g. perihilar, anterior), particularly at centers without expertise in performing these procedures. Alternatively, mpMRI would potentially avoid additional procedures, and the lack of invasiveness might encourage provider utilization.

The issue of false-positives was most notable with oncocytomas, emphasizing the challenge in differentiating it from ccRCC. Similarly, Cornelis and colleagues noted difficulty in their retrospective evaluation as two radiologists blinded to final pathology had a diagnostic specificity of 94%, but only 19% sensitivity, in distinguishing ccRCC from oncocytoma.¹² Similarly, Rosenkrantz et al. found no MRI features that would allow differentiation of oncocytoma from chromophobe RCC using a standard clinical MRI protocol similar to the mpMRI protocols in our study.²⁸ Further studies, specifically with arterial spin labeling (ASL), may have the potential to separate oncocytomas and ccRCC. Although not currently commercially available, this technique labels the spin of arterial water allowing, in effect, contrasted imaging without intravenous tracers.²⁹ Prior work has shown significant differences in mean ASL perfusion levels of oncocytoma and ccRCC.³⁰ Adding this technique to the mpMRI algorithm may further improve diagnostic accuracy.

As highlighted above, most studies regarding mpMRI involve at most a few reviewing radiologists.^{7,12} To our knowledge, we are the first to evaluate inter-reader variability among a large cohort of radiologists. The seven readers in our series had varying levels experience, ranging from in-fellowship training to senior faculty (1–15 years) and we found that radiologist level of experience did not appear to correlate with ccLS accuracy. The reason for this is speculative, but might be a reflection of more recent emphasis on mpMRI exposure in residency and fellowship programs. Additionally, the structured algorithm might mitigate some effects of experience. As for inter-reader variability, we demonstrated good consistency (mean weighted κ 0.53) among our radiologists when utilizing the algorithm and ccLS scoring. However, this also highlights opportunity for improvement. Given the multitude of adjustable parameters with mpMRI, inter-center standardization is needed to specify imaging protocols that will best characterize SRM.

Our study has limitations that deserve mention. First is the retrospective design. While our radiologists were blinded to final pathology, this structure has inherent bias. Not all patients with SRM undergo mpMRI, so there is selection bias that could affect our estimates of RMB (ccLS 3, 20%) or unnecessary ccLS 4–5 surgery (6.2%) in this series. In addition, not all patients who had mpMRI underwent surgery. This selection bias limits our ability to capture benign appearing lesions, which could also affect our accuracy. Therefore, the strength of this modality will ultimately depend on a prospective analysis to verify that ccLS can accurately direct SRM management. Second is the single-institution series. As stated previously, all mpMRI sequences are not equal, and standardization is required to improve inter-center reproducibility. However, the reasonable diagnostic accuracy of the ccLS considering the multiple mpMRI studies performed at different institutions with different imaging protocols is encouraging. Future studies should be multi-institutional to ensure stability of results between various centers. Third, our study is small with a cohort of only 121 SRM, of which 61 were ccRCC. However, in comparison to other discussed series,

7,12,13 we do report the largest SRM series to date. Larger series are ultimately needed to define the accuracy of this work.

These limitations notwithstanding, we have demonstrated that ccLS can accurately predict ccRCC in cT1a renal masses. In addition to providing anatomic information for surgical planning, this could streamline SRM decision-making and obviate the need for additional procedures prior to definitive management. Moreover, our reported technique has good inter-reader variability. With future prospective and multi-institutional studies we hope to verify these initial results and the generalizability of this technique.

Acknowledgments

Extra-institutional funding: SPOR grant #P50CA196516; partially funded by grant #5RO1CA154475

References

1. Frank I, Blute ML, Cheville JC, et al. Solid renal tumors: an analysis of pathological features related to tumor size. *J Urol.* 2003; 170:2217–2220. [PubMed: 14634382]
2. Kutikov A, Smaldone MC, Uzzo RG, et al. Renal Mass Biopsy: Always, Sometimes, or Never? *Eur Urol.* 2016; 70:403–406. [PubMed: 27085625]
3. Tomaszewski JJ, Uzzo RG, Smaldone MC. Heterogeneity and renal mass biopsy: a review of its role and reliability. *Cancer Biol Med.* 2014; 11:162–172. [PubMed: 25364577]
4. Leppert JT, Hanley J, Wagner TH, et al. Utilization of renal mass biopsy in patients with renal cell carcinoma. *Urology.* 2014; 83:774–779. [PubMed: 24529579]
5. Breau RH, Crispen PL, Jenkins SM, et al. Treatment of patients with small renal masses: a survey of the American Urological Association. *J Urol.* 2011; 185:407–413. [PubMed: 21168170]
6. Patel HD, Johnson MH, Pierorazio PM, et al. Diagnostic Accuracy and Risks of Biopsy in the Diagnosis of a Renal Mass Suspicious for Localized Renal Cell Carcinoma: Systematic Review of the Literature. *J Urol.* 2016; 195:1340–1347. [PubMed: 26901507]
7. Pedrosa I, Chou MT, Ngo L, et al. MR classification of renal masses with pathologic correlation. *Eur Radiol.* 2008; 18:365–375. [PubMed: 17899106]
8. Ramamurthy NK, Moosavi B, McInnes MDF, et al. Multiparametric MRI of solid renal masses: pearls and pitfalls. *Clin Radiol.* 2015; 70:304–316. [PubMed: 25472466]
9. Allen BC, Tirman P, Clingan MJ, et al. Characterizing solid renal neoplasms with MRI in adults. *Abdom Imaging.* 2014; 39:358–387. [PubMed: 24446014]
10. Pedrosa I, Sun MR, Spencer M, et al. MR imaging of renal masses: correlation with findings at surgery and pathologic analysis. *Radiographics.* 2008; 28:985–1003. [PubMed: 18635625]
11. Sun MRM, Ngo L, Genega EM, et al. Renal cell carcinoma: dynamic contrast-enhanced MR imaging for differentiation of tumor subtypes—correlation with pathologic findings. *Radiology.* 2009; 250:793–802. [PubMed: 19244046]
12. Cornelis F, Tricaud E, Lasserre AS, et al. Routinely performed multiparametric magnetic resonance imaging helps to differentiate common subtypes of renal tumours. *Eur Radiol.* 2014; 24:1068–1080. [PubMed: 24557052]
13. Hötter AM, Mazaheri Y, Wibmer A, et al. Differentiation of Clear Cell Renal Cell Carcinoma From Other Renal Cortical Tumors by Use of a Quantitative Multiparametric MRI Approach. *AJR Am J Roentgenol.* 2017; 208:W85–W91. [PubMed: 28095036]
14. Vargas HA, Chaim J, Lefkowitz RA, et al. Renal cortical tumors: use of multiphasic contrast-enhanced MR imaging to differentiate benign and malignant histologic subtypes. *Radiology.* 2012; 264:779–788. [PubMed: 22829683]
15. Störkel S, Eble JN, Adlaka K, et al. Classification of renal cell carcinoma: Workgroup No. 1. Union Internationale Contre le Cancer (UICC) and the American Joint Committee on Cancer (AJCC). *Cancer.* 1997; 80:987–989. [PubMed: 9307203]

16. Outwater EK, Bhatia M, Siegelman ES, et al. Lipid in renal clear cell carcinoma: detection on opposed-phase gradient-echo MR images. *Radiology*. 1997; 205:103–107. [PubMed: 9314970]
17. Jhaveri KS, Elmi A, Hosseini-Nik H, et al. Predictive Value of Chemical-Shift MRI in Distinguishing Clear Cell Renal Cell Carcinoma From Non-Clear Cell Renal Cell Carcinoma and Minimal-Fat Angiomyolipoma. *AJR Am J Roentgenol*. 2015; 205:W79–86. [PubMed: 26102422]
18. Yoshimitsu K, Honda H, Kuroiwa T, et al. MR detection of cytoplasmic fat in clear cell renal cell carcinoma utilizing chemical shift gradient-echo imaging. *J Magn Reson Imaging*. 1999; 9:579–585. [PubMed: 10232518]
19. Hindman N, Ngo L, Genega EM, et al. Angiomyolipoma with minimal fat: can it be differentiated from clear cell renal cell carcinoma by using standard MR techniques? *Radiology*. 2012; 265:468–477. [PubMed: 23012463]
20. Costa DN, Lotan Y, Rofsky NM, et al. Assessment of Prospectively Assigned Likert Scores for Targeted Magnetic Resonance Imaging-Transrectal Ultrasound Fusion Biopsies in Patients with Suspected Prostate Cancer. *J Urol*. 2016; 195:80–87. [PubMed: 26192254]
21. Park SY, Jung DC, Oh YT, et al. Prostate Cancer: PI-RADS Version 2 Helps Preoperatively Predict Clinically Significant Cancers. *Radiology*. 2016; 280:108–116. [PubMed: 26836049]
22. Moch H, Cubilla AL, Humphrey PA, et al. The 2016 WHO Classification of Tumours of the Urinary System and Male Genital Organs-Part A: Renal, Penile, and Testicular Tumours. *Eur Urol*. 2016; 70:93–105. [PubMed: 26935559]
23. Kang SK, Zhang A, Pandharipande PV, et al. DWI for Renal Mass Characterization: Systematic Review and Meta-Analysis of Diagnostic Test Performance. *AJR Am J Roentgenol*. 2015; 205:317–324. [PubMed: 26204281]
24. Kay FU, Pedrosa I. Imaging of Solid Renal Masses. *Radiol Clin North Am*. 2017; 55:243–258. [PubMed: 28126214]
25. Sasiwimonphan K, Takahashi N, Leibovich BC, et al. Small (<4 cm) renal mass: differentiation of angiomyolipoma without visible fat from renal cell carcinoma utilizing MR imaging. *Radiology*. 2012; 263:160–168. [PubMed: 22344404]
26. Frank I, Blute ML, Chevillat JC, et al. An outcome prediction model for patients with clear cell renal cell carcinoma treated with radical nephrectomy based on tumor stage, size, grade and necrosis: the SSIGN score. *J Urol*. 2002; 168:2395–2400. [PubMed: 12441925]
27. Halverson SJ, Kunju LP, Bhalla R, et al. Accuracy of Determining Small Renal Mass Management with Risk Stratified Biopsies: Confirmation by Final Pathology. *J Urol*. 2013; 189:441–446. [PubMed: 23253955]
28. Rosenkrantz AB, Hindman N, Fitzgerald EF, et al. MRI features of renal oncocytoma and chromophobe renal cell carcinoma. *AJR Am J Roentgenol*. 2010; 195:W421–7. [PubMed: 21098174]
29. Pedrosa I, Rafatzand K, Robson P, et al. Arterial spin labeling MR imaging for characterisation of renal masses in patients with impaired renal function: initial experience. *Eur Radiol*. 2012; 22:484–492. [PubMed: 21877173]
30. Lanzman RS, Robson PM, Sun MR, et al. Arterial spin-labeling MR imaging of renal masses: correlation with histopathologic findings. *Radiology*. 2012; 265:799–808. [PubMed: 23047841]

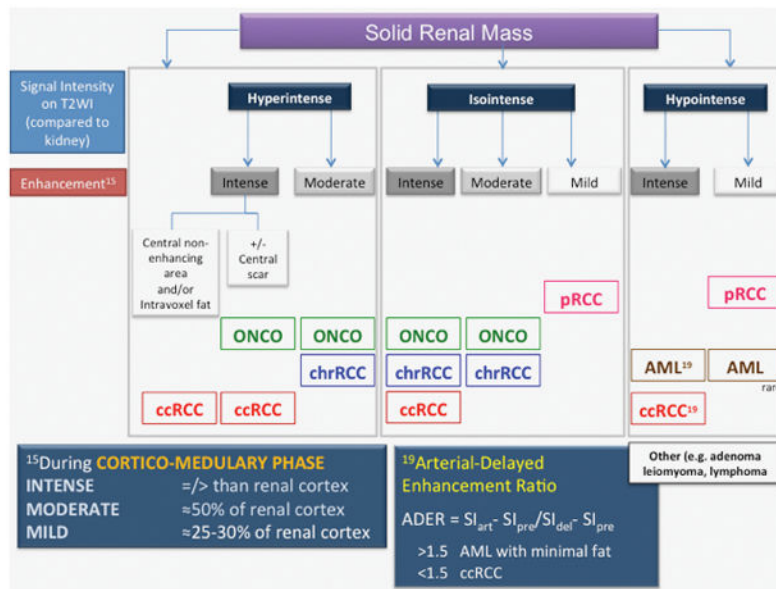


Figure 1. Multiparametric MRI algorithm for small renal masses. ccRCC- clear cell renal cell carcinoma. chrRCC- chromophobe renal cell carcinoma. pRCC- papillary renal cell carcinoma. ONCO- oncocytoma. AML- angiomyolipoma. SI- signal intensity. Reprinted from Radiologic Clinics of North America, Volume 55, Issue 2, Kay FU and Pedrosa I, “Imaging of Solid Renal Masses,” pg 243–258, Copyright 2017, with permission from Elsevier.

Author Manuscript

Author Manuscript

Author Manuscript

Author Manuscript

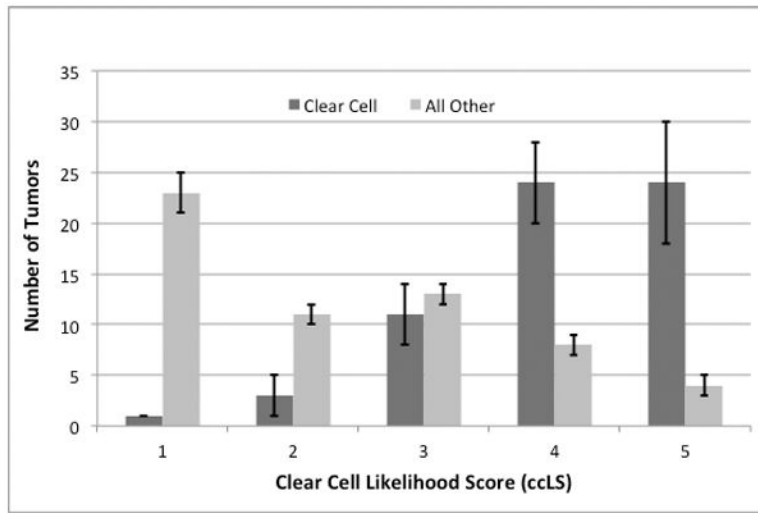


Figure 2. Histologic distribution of the entire cohort by clear cell likelihood score. Tumors that could not be assessed are not shown.

Author Manuscript

Author Manuscript

Author Manuscript

Author Manuscript

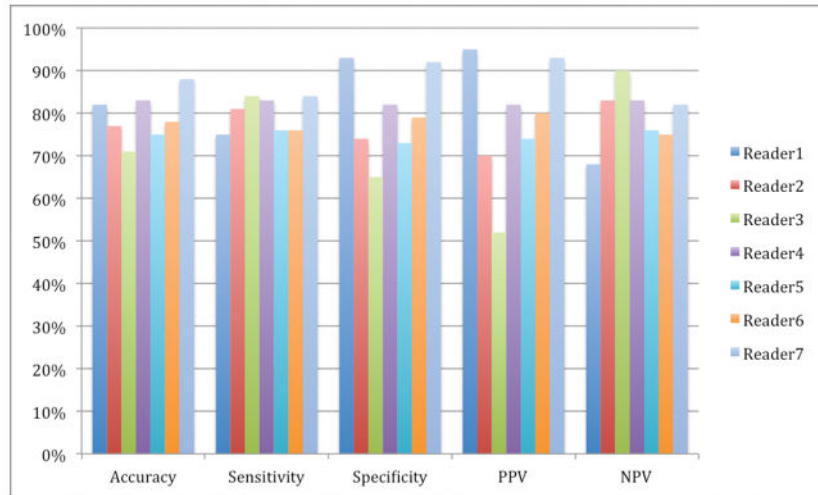


Figure 3. Binary classification of the seven readers defining clear cell RCC as ccLS 4–5. RCC- renal cell carcinoma. ccLS- clear cell likelihood score.

Author Manuscript

Author Manuscript

Author Manuscript

Author Manuscript

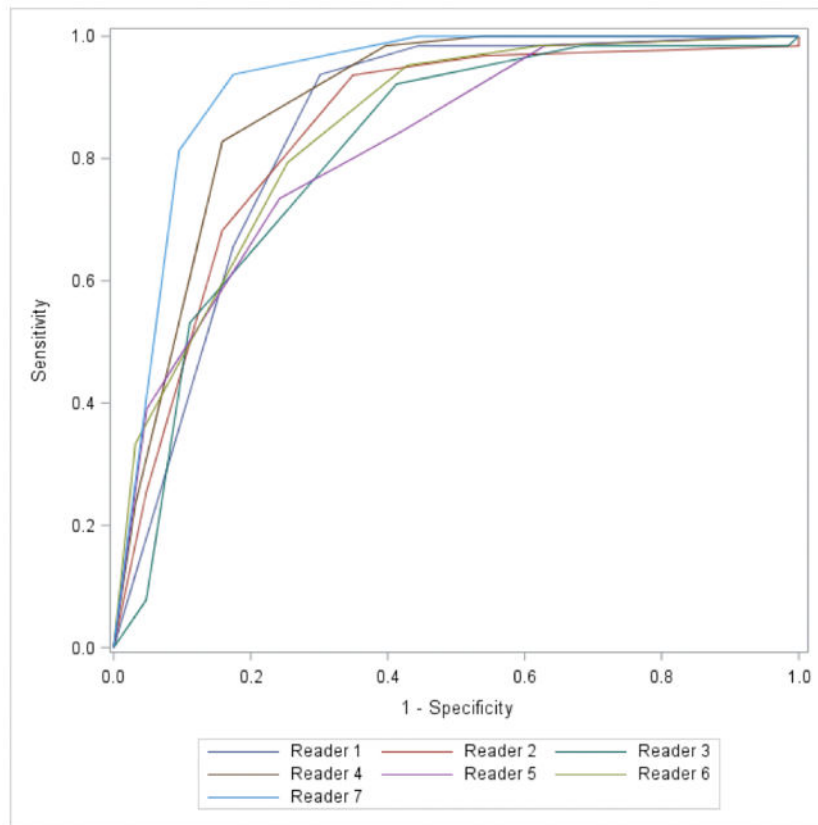


Figure 4. Receiver operating characteristic curves of the seven readers defining ccRCC and ccLS 4–5. RCC- renal cell carcinoma. ccLS- clear cell likelihood score.

Table 1

Patient demographics and final pathology. SD= standard deviation, RCC= renal cell carcinoma.

	n= 110 patients (121 tumors)
Age, y (mean \pm SD)	57 \pm 14
Male/Female (%)	61/39%
Tumor size, cm (mean \pm SD)	2.4 \pm 0.8
Histology (%)	
Clear cell RCC	61 (50%)
Papillary RCC	25 (21%)
Chromophobe RCC	9 (7%)
Other RCC	6 (5%)
Oncocytoma	7 (6%)
Angiomyolipoma	6 (5%)
Other benign	7 (6%)
Final pathology	
pT1a	97 (96%)
pT3a	4 (4%)
Fuhrman Grade	
1	6 (6%)
2	72 (71%)
3	15 (15%)
4	0
Unknown	8 (8%)

Mean percentage according to histologic subtype versus clear cell likelihood score. Values in each cell represent column percentage within each histology, while numbers in parenthesis indicate the mean number of renal masses across all readers. ccLS- clear cell likelihood score, RCC- renal cell carcinoma, AML- angiomyolipoma.

Table 2

ccLS	Clear cell RCC	Papillary RCC	Chromophobe RCC	Oncocytoma	Lipid-poor AML	Other
1- Definitely not	0.7% (0.4)	66.1% (16.6)	20.9% (1.9)	0.0%	29.7% (1.9)	13.0% (1.7)
2- Probably not	3.8% (2.3)	20.3% (5.1)	15.4% (1.4)	27.1% (1.9)	15.7% (1.0)	12.2% (1.6)
3- Equivocal	17.3% (10.6)	5.6% (1.4)	48.4% (4.4)	34.3% (2.4)	25.0% (1.6)	25.2% (3.3)
4- Probably	38.8% (23.7)	4.0% (1.0)	11.0% (1.0)	24.3% (1.7)	9.4% (0.6)	27.5% (3.6)
5- Definitely	38.6% (23.6)	1.2% (0.3)	0.0%	14.3% (1.0)	4.7% (0.3)	20.6% (2.7)
Cannot be assessed	0.8% (0.5)	2.8% (0.7)	4.4% (0.4)	0.0%	15.6% (1.0)	1.5% (0.2)